- A surfactant-assisted unimolecular platform for multicolor emissions
  Zhao, L.; Cheng, X.; Ding, Y.; Yan, Y.; Huang, J. *Soft Matter* **2012**, *8*, 10472-10478.
  Abstract:

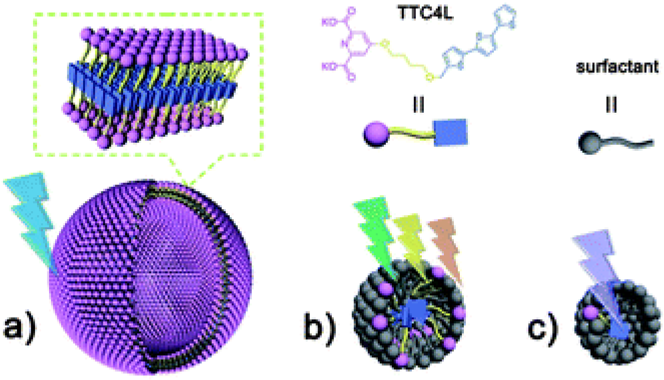

We present here a simple molecular assembly approach to multicolor emissions based on a unimolecular platform of a terthiophene-containing amphiphile TTC4L. The amphiphiles self-assemble into vesicles in solution which exhibit a blue emission. Upon controlling the distance between the fluorescent terthiophene groups by transformation of the self-assembly of TTC4L molecules into their co-assembly with surfactants, the color of the emissions can be continuously tailored which covers most of the visible region. Since the multi-colors were obtained without any structural modification on the fluorescent molecules, we have demonstrated a real unimolecular platform for fabricating multicolor emissions. In contrast, only dual emissions can be obtained from TTC4L using host–guest chemistry. As a simple approach of ‘tunable emissions’, this surfactant-assisted unimolecular platform opens a new vista for the application of molecular assemblies in advanced light emitting materials.

- Synthesis and self-assembly of nonamphiphilic hyperbranched polyoximes
  Jin, Y.; Song, L.; Wang, D.; Qiu, F.; Yan, D.; Zhu, B.; Zhu, X. *Soft Matter* **2012**, *8*, 10017-10025.
  Abstract:

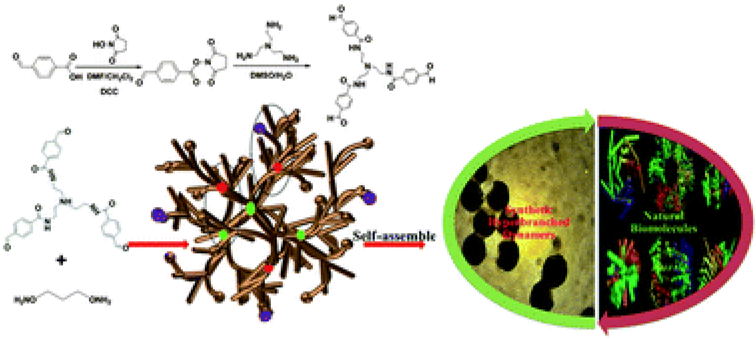

Nonamphiphilic hyperbranched polyoximes (HPOXs) were successfully synthesized by the polycondensation of trialdehyde and bis-aminooxy monomers with different molar feeding ratios. Various characterization techniques, such as 1D and 2D nuclear magnetic resonance (NMR), Fourier transform infrared spectroscopy (FTIR), and multi-detector gel permeation chromatography (GPC) were used to identify the highly branched structure of the HPOXs. Despite there being no amphiphilic block segments, HPOXs with a torispherical structure could self-assemble into nanoparticles in a mixed solution of dimethyl sulfoxide and H_2O. Besides, the modulation of the degree of branching (DB) and the terminal groups resulted in the appearance of spherical and bowl-shaped morphologies due to the change of the intra- and inter-molecular interactions. Accordingly, dynamic light scattering

(DLS), transmission electron microscopy (TEM), atomic force microscopy (AFM), scanning electron microscopy (SEM), fluorescence spectroscopy (FL) together with ultraviolet and visible spectrometery (UV-vis) were employed to unravel the tentative mechanism of the formation of the HPOX self-assemblies. Moreover, dynamic oxime linkages and hydrogen bonds endowed the HPOX nanoparticles with pH and thermal dual responsiveness, which was confirmed by TEM measurements. HPOXs are developed to offer a novel pathway for the design of nonamphiphilic self-assemblies with dual responsiveness.

- Preparation of Synthetically Challenging Nucleotides Using Cyanoethyl P-Imidazolides and Microwaves
  Strenkowska, M.; Wanat, P.; Ziemniak, M.; Jemielity, J.; Kowalska, J. *Org. Lett.* **2012**, *14*, 4782–4785.
  Abstract:

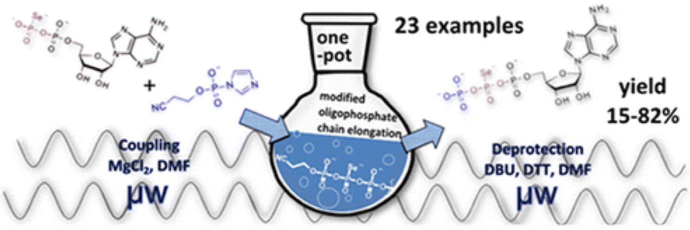

We describe a general method for the elongation of nucleoside oligophosphate chains by means of cyanoethyl (CE) phosphorimidazolides. Though the method requires a phosphorylation and subsequent deprotection reaction, both steps could be achieved in one pot without isolation/purification of the initial phosphorylation product. We have also found that pyrophosphate bond formation by this method is significantly accelerated by microwave irradiation.

- Total Synthesis of (+)-Aureol
  Kuan, K. K. W.; Pepper, H. P.; Bloch, W. M.; George, J. H. *Org. Lett.* **2012**, *14*, 4710–4713.
  Abstract:

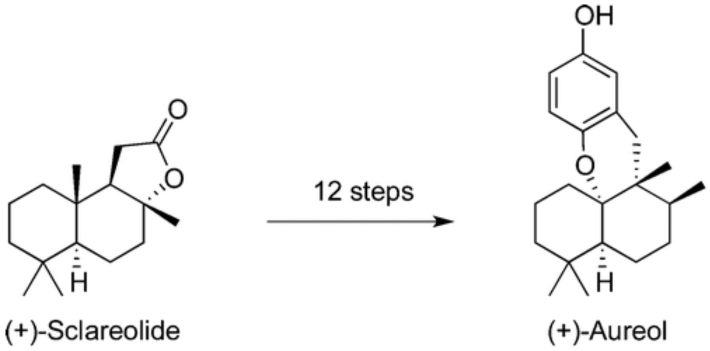

A total synthesis of the marine sponge meroterpenoid (+)-aureol has been achieved in 12 steps (6% overall yield) from (+)-sclareolide. Key steps of the synthesis include a biosynthetically inspired sequence of 1,2-hydride and methyl shifts, and a biomimetic cycloetherification reaction.

- An Amphiphilic Pillar[5]arene: Synthesis, Controllable Self-Assembly in Water, and Application in Calcein Release and TNT Adsorption
  Yao, Y.; Xue, M.; Chen, J.; Zhang, M.; Huang, F. *J. Am. Chem. Soc.* **2012**, *134*, 15712–15715.
  Abstract:

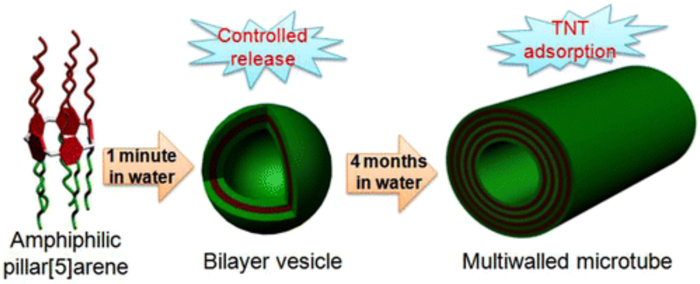

An amphiphilic pillar[5]arene was made. It could self-assemble to form vesicles and multiwalled microtubes in water. Dynamic light scattering, transmission electron microscopy, scanning electron microscopy, atomic force microscopy, and UV–vis and FTIR spectroscopy were employed to characterize its self-assembly process and the resultant assemblies. The vesicles could encapsulate calcein within their interiors under neutral conditions and release it in response to a decrease in pH. The microtubes, which have primary amine groups on their surfaces, could adsorb TNT through donor–acceptor interactions.

- Single-walled Carbon Nanotube Growth from Chiral Carbon Nanorings: Prediction of Chirality and Diameter Influence on Growth Rates
  Li, H.-B.; Page, A. J.; Irle, S.; Morokuma, K. *J. Am. Chem. Soc.* **2012**, *134*, 15887–15896.
  Abstract:

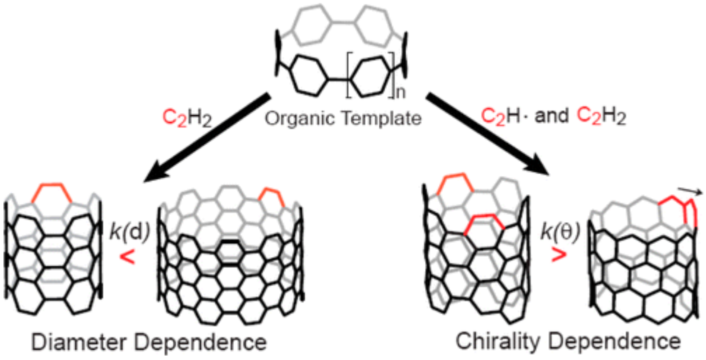

Catalyst-free, chirality-controlled growth of chiral and zigzag single-walled carbon nanotubes (SWCNTs) from organic precursors is demonstrated using quantum chemical simulations. Growth of (4,3), (6,5), (6,1), (10,1) and (8,0) SWCNTs was induced by ethynyl radical (C2H) addition to organic precursors. These simulations show a strong dependence of the SWCNT growth rate on the chiral angle, θ. The SWCNT diameter however does not influence the SWCNT growth rate under these conditions. This agreement with a previously proposed screw-dislocation-like model of transition metal-catalyzed SWCNT growth rates indicates that the SWCNT growth rate is an intrinsic property of the SWCNT edge itself. Conversely, we predict that the rate of SWCNT growth via Diels–Alder cycloaddition of C2H2 is strongly influenced by the diameter of the SWCNT. We therefore predict the existence of a maximum growth rate for an optimum diameter/chirality combination at a given C2H/C2H2 ratio. We also find that the ability of a SWCNT to avoid defect formation during growth is an intrinsic quality of the SWCNT edge.

- Structural and Conformational Dynamics of Self-Assembling Bioactive β-Sheet Peptide Nanostructures Decorated with Multivalent RNA-Binding Peptides
  Han, S.; Kim, D.; Han, S.-H.; Kim, N. H.; Kim, S. H.; Lim, Y.-B. *J. Am. Chem. Soc.* **2012**, *134*, 16047–16053.

Abstract:

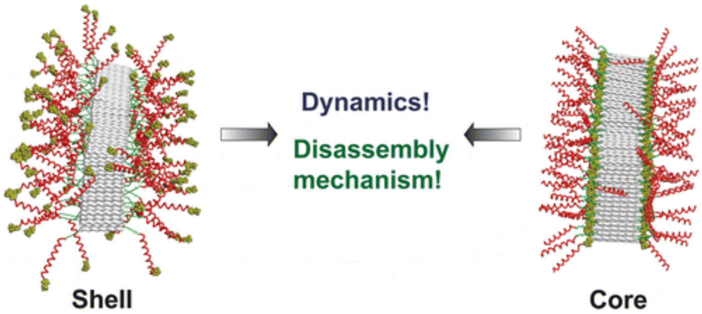

Understanding the dynamic behavior of nanostructural systems is important during the development of controllable and tailor-made nanomaterials. This is particularly true for nanostructures that are intended for biological applications because biomolecules are usually highly dynamic and responsive to external stimuli. In this Article, we investigated the structural and conformational dynamics of self-assembling bioactive β-sheet peptide nanostructures using electron paramagnetic resonance (EPR) spectroscopy. The model peptide nanostructures are characterized by the cross-β spine of β-ribbon fibers and multiple RNA-binding bioactive peptides that constitute the shell of the nanostructures. We found first, that bioactive peptides at the shell of β-ribbon nanostructure have a mobility similar to that of an isolated monomeric peptide. Second, the periphery of the cross-β spine is more immobile than the distal part of surface-displayed bioactive peptides. Third, the rotational dynamics of short and long fibrils are similar; that is, the mobility is largely independent of the extent of aggregation. Fourth, peptides that constitute the shell are affected first by the external environment at the initial stage. The cross-β spine resists its external environment to a certain extent and abruptly disintegrates when the perturbation reaches a certain degree. Our results provide an overall picture of β-sheet peptide nanostructure dynamics, which should be useful in the development of dynamic self-assembled peptide nanostructures.

- Engineered Synthetic Polymer Nanoparticles as IgG Affinity Ligands
  Lee, S.-H.; Hoshino, Y.; Randall, A.; Zeng, Z.; Baldi, P.; Doong, R.-A.; Shea, K. J. *J. Am. Chem. Soc.* **2012**, *134*, 15765–15772.
  Abstract:

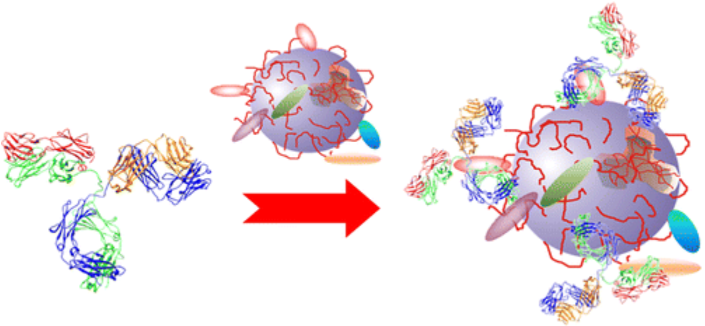

A process for the preparation of an abiotic protein affinity ligand is described. The affinity ligand, a synthetic polymer hydrogel nanoparticle (NP), is formulated with functional groups complementary to the surface presentation of the target protein. An iterative process is used to improve affinity by optimizing the composition and proportion of functional monomers. Since the polymer NPs are formed by a kinetically driven process, the sequence of functional monomers in the polymer chain is not controlled; only the average composition can be adjusted by the stoichiometry of the monomers in the feed. To compensate for this the hydrogel NP is lightly cross-linked resulting in chain flexibility that takes place on a submillisecond time scale allowing the polymer to “map” onto a protein surface with complementary functionality. In this study, we report a lightly cross-linked (2%) N-isopropyl acrylamide (NIPAm) synthetic polymer NP (50–65 nm) incorporating hydrophobic and carboxylate groups that binds with high affinity to the Fc fragment of IgG. The affinity and amount of NP bound to IgG is pH dependent. The hydrogel NP inhibits protein A binding to the Fc domain at pH 5.5, but not at pH 7.3. A computational analysis was used to identify potential NP–protein interaction sites. Candidates include a NP binding domain that overlaps with the protein A–Fc binding domain at pH 5.5. The computational analysis supports the inhibition experimental results and is attributed to the difference in the charged state of histidine residues. Affinity of the NP (3.5–8.5 nM) to the Fc domain at pH 5.5 is comparable to protein A at pH 7. These results establish that engineered synthetic polymer NPs can be formulated with an intrinsic affinity to a specific domain of a large biomacromolecule.

- Gold-Catalyzed Direct Arylation.
  Ball, L. T.; Lloyd-Jones, G. C.; Russell, C. A. *Science* **2012**, *337*, 1644-1648.
  Abstract:

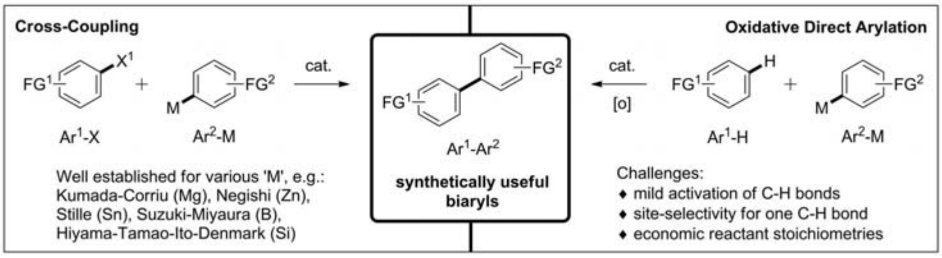

Biaryls (two directly connected aromatic rings, Ar^1-Ar^2) are common motifs in pharmaceuticals, agrochemicals, and organic materials. Current methods for establishing the Ar^1-Ar^2 bond are dominated by the cross-coupling of aryl halides (Ar^1-X) with aryl metallics (Ar^2-M). We report that, in the presence of 1 to 2 mole percent of a gold catalyst and a mild oxidant, a wide range of arenes (Ar^1-H) undergo site-selective arylation by arylsilanes (Ar^2-$SiMe_3$) to generate biaryls (Ar^1-Ar^2), with little or no homocoupling (Ar^1-Ar^1/Ar^2-Ar^2). Catalysis proceeds at room temperature and tolerates a broad range of functional groups, including those incompatible with cross-coupling. These features expedite biaryl preparation, as demonstrated by synthesis of the nonsteroidal anti-inflammatory diflunisal.

- Quantum Junction Solar Cells
  Tang, J.; Liu, H.; Zhitomirsky, D.; Hoogland, S.; Wang, X.; Furukawa, M.; Levina, L.; Sargent, E. H. *Nano Letters* **2012**, *12*, 4889-4894.
  Abstract:

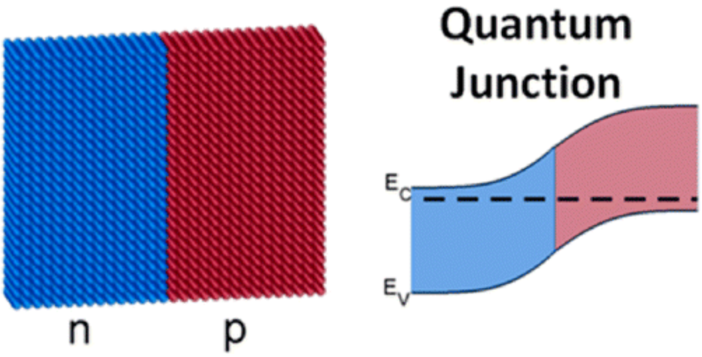

Colloidal quantum dot solids combine convenient solution-processing with quantum size effect tuning, offering avenues to high-efficiency multijunction cells based on a single materials synthesis and processing platform. The highest-performing colloidal quantum dot rectifying devices reported to date have relied on a junction between a quantum-tuned absorber and a bulk material (e.g., TiO_2); however, quantum tuning of the absorber then requires complete redesign of the bulk acceptor, compromising the benefits of facile quantum tuning. Here we report rectifying junctions constructed entirely using inherently band-aligned quantum-tuned materials. Realizing these quantum junction diodes relied upon the creation of an n-type quantum dot solid having a clean bandgap. We combine stable, chemically compatible, high-performance n-type and p-type materials to create the first quantum junction solar cells. We present a family of photovoltaic devices having widely tuned bandgaps of 0.6–1.6 eV that excel where conventional quantum-to-bulk devices fail to perform. Devices having optimal single-junction bandgaps exhibit certified AM1.5 solar power conversion efficiencies of 5.4%. Control over doping in quantum solids, and the successful integration of these materials to form stable quantum junctions, offers a powerful new degree of freedom to colloidal quantum dot optoelectronics.

- A Synthetic Chemomechanical Machine Driven by Ligand–Receptor Bonding
  Lavella, G. J.; Jadhav, A. D.; Maharbiz, M. M. *Nano Letters* **2012**, *12*, 4983-4987.
  Abstract:

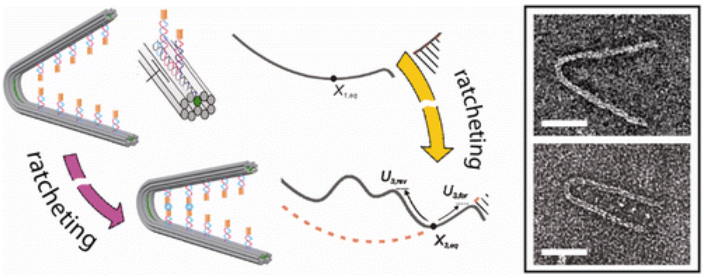

The ability to create synthetic chemomechanical machines with engineered functionality promises large technological rewards. However, current efforts in molecular chemistry are restrained by the formidable challenges faced in molecular structure and function prediction. An alternative approach to engineering machines with tailorable chemomechanical functionality is to design Brownian ratchet devices using molecular assemblies. We demonstrate this through the creation of autonomous molecular machines that sense, mechanically react, and extract energy from ligand–receptor binding. We present a specific instantiation, measuring approximately 100 nm in length, which actuates upon detection of a streptavidin ligand. Machines were designed through the tailoring of energy landscapes on 3D DNA origami motifs. We also analyzed the response over a logarithmic concentration ratio (device:ligand) range from $1:10^1$ to $1:10^5$.

- Charge Transport in Poly(3-butylthiophene) Nanowires and Their Nanocomposites with an Insulating Polymer
  Kim, F. S.; Jenekhe, S. A. *Macromolecules* **2012**, *45*, 7514–7519.
  Abstract:

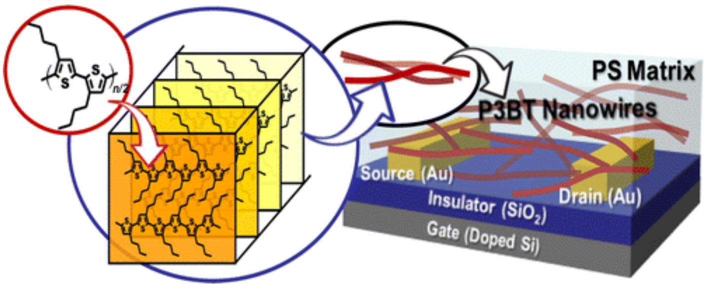

Self-assembled crystalline nanowires (NWs) of poly(3-butylthiophene) (P3BT), having an average width of 11.8 nm and aspect ratios of ~330–850, and their nanocomposites with insulating polystyrene (PS) were found to have a high field-effect mobility of holes and a high dc conductivity. The intra-nanowire carrier mobility in the P3BT-NW/PS nanocomposites can be as high as 0.2 $cm^2 V^{-1} s^{-1}$, which is significantly enhanced compared to films of pure P3BT NWs. Nanocomposites of P3BT NWs with polystyrene were found to support high carrier densities (10^{17}–10^{18} cm^{-3}) with high mobility of holes, facilitating the development of high performance field-effect transistors. The observed high carrier mobility and high conductivity in the nanocomposites were explained by the rather low percolation threshold (0.5 wt % P3BT NWs).

- How Structure-Related Collapse Mechanisms Determine Nanoscale Inhomogeneities in Thermoresponsive Polymers
  Kurzbach, D.; Schömer, M.; Wilms, V. S; Frey, H.; Hinderberger, D. *Macromolecules* **2012**, *45*, 7535–7548.
  Abstract:

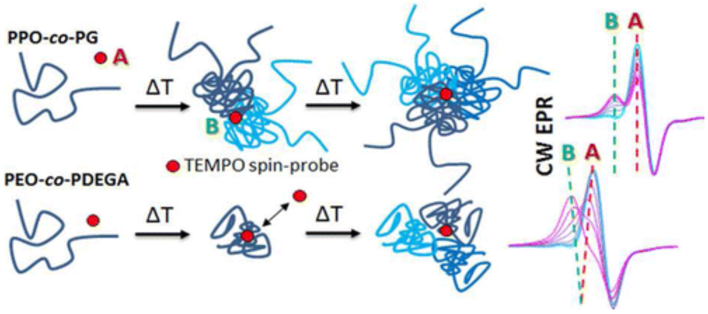

Continuous wave electron paramagnetic resonance (CW EPR) spectroscopy on the amphiphilic spin probe TEMPO in solutions of selectively chosen functional, thermoresponsive poly(propylene oxide) (PPO)- and poly(ethylene oxide) (PEO)-based copolymers of both linear and branched structure is used to elucidate their host–guest interactions and inverse phase transitions. Three different fundamental types of host–guest interactions between probes and polymers could be correlated to the phase transition mechanisms (supported by MD simulations), evidencing that these proceed via nanoscale inhomogeneities of the polymers. Because of their ability to host small amphiphilic guest molecules, thermoresponsive copolymers are promising candidates for molecular transport applications. The host–guest interaction principles derived from our small amphiphilic spin probes may also aid in finding the "appropriate" design for the desired release property of a specific thermoresponsive polymer-based host–guest systems.

- A Selenium-Based Cathode for a High-Voltage Tandem Photoelectrochemical Solar Cell
  Qian, J.; Jiang, K.-J.; Huang, J.-H.; Liu, Q.-S.; Yang, L.-M.; Song, Y. *Angew. Chem. Int. Ed.* **2012**, *51*, 10351-10354.

Abstract:

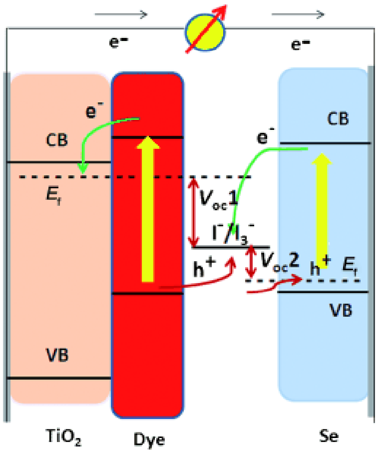

High voltage: A selenium-based photocathode has been developed for a photoelectrochemical solar cell with a high open-circuit voltage Voc of 318 mV and an efficiency of 0.34 %. A higher Voc of 940 mV was realized in a tandem solar cell with a conventional N719 dye-sensitized photoanode, giving an efficiency of 0.98 %.

- Self-Cleaning Functional Molecular Materials
  Avinash, M. B.; Verheggen, E.; Schmuck, C.; Govindaraju, T. *Angew. Chem. Int. Ed.* **2012**, *51*, 10324-10328.
  Abstract:

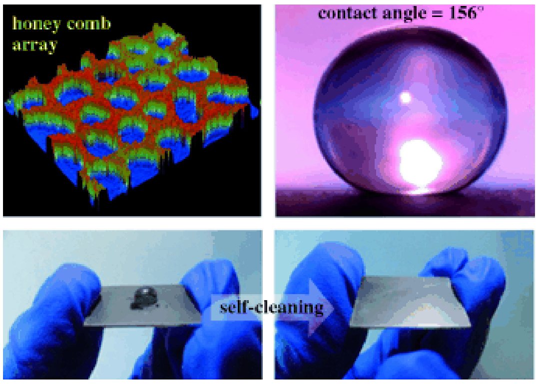

Clean and polish: The spontaneous hierarchical molecular assembly of a naphthalenediimide derivative is used to form microarrays by a simple solution-processing technique. This method is further employed to fabricate a self-cleaning surface with very low slide angle (3°) and contact angle hysteresis (1°).

- Charge-Transfer Interactions in Tris-Donor–Tris-Acceptor Hexaarylbenzene Redox Chromophores
  Steeger, M.; Lambert, C. *Chem. Eur. J.* **2012**, *18*, 11937 – 11948.
  Abstract:

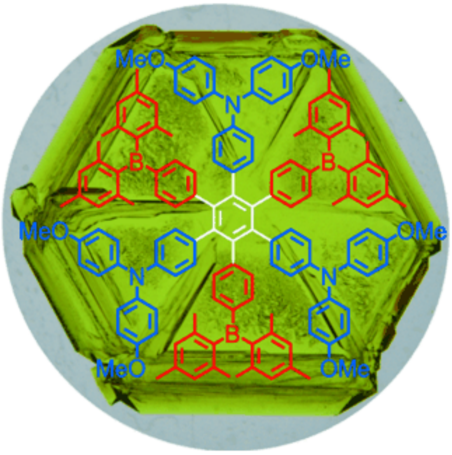

Symmetric- and asymmetric hexaarylbenzenes (HABs), each substituted with three electron-donor triarylamine redox centers and three electron-acceptor triarylborane redox centers, were synthesized by cobalt-catalyzed cyclotrimerization, thereby forming compounds with six- and four donor–acceptor interactions, respectively. The electrochemical- and photophysical properties of these systems were investigated by cyclovoltammetry (CV), as well as by absorption- and fluorescence spectroscopy, and compared to a HAB that only contained one neighboring donor–acceptor pair. CV measurements of the asymmetric HAB show three oxidation peaks and three reduction peaks, whose peak-separation is greatly influenced by the conducting salt, owing to ion-pairing and shielding effects. Consequently, the peak-separations cannot be interpreted in terms of the electronic couplings in the generated mixed-valence species. Transient-absorption spectra, fluorescence-solvatochromism, and absorption spectra show that charge-transfer states from the amine- to the boron centers are generated after optical excitation. The electronic donor–acceptor interactions are weak because the charge transfer has to occur predominantly through space. Moreover, the excitation energy of the localized excited charge-transfer states can be redistributed between the aryl substituents of these multidimensional chromophores within the fluorescence lifetime (about 60 ns). This result was confirmed by steady-state fluorescence-anisotropy measurements, which further indicated symmetry-breaking in the superficially symmetric HAB. Adding fluoride ions causes the boron centers to lose their accepting ability owing to complexation. Consequently, the charge-transfer character in the donor–acceptor chromophores vanishes, as observed in both the absorption- and fluorescence spectra. However, the ability of the boron center as a fluoride sensor is strongly influenced by the moisture content of the solvent, possibly owing to the formation of hydrogen-bonding interactions between water molecules and the fluoride anions.

- High-Performance Dipolar Organic Dyes with an Electron-Deficient Diphenylquinoxaline Moiety in the π-Conjugation Framework for Dye-Sensitized Solar Cells
  Li, S.-R.; Lee, C.-P.; Kuo, H.-T.; Ho, K.-C.; Sun, S.-S. *Chem. Eur. J.* **2012**, *18*, 12085 – 12095.
  Abstract:

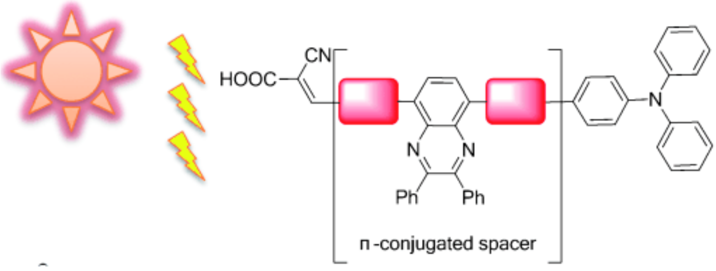

We report here the synthesis and electrochemical and photophysical properties of a series of easily prepared dipolar organic dyes and their application in dye-sensitized solar cells (DSSCs). For the six organic dyes, the molecular structures comprised a triphenylamine group as an electron donor, a cyanoacrylic acid as an electron acceptor, and an electron-deficient diphenylquinoxaline moiety integrated in the π-conjugated spacer between the electron donor and acceptor moieties. The incorporation of the electron-deficient diphenylquinoxaline moiety effectively reduces the energy gap of the dyes and broadly extends the spectral coverage. DSSCs based on dye 6 produced the best overall cell performance of 7.35 %, which translates to approximately 79 % of the intrinsic efficiency of the DSSCs based on the standard N719 dye under identical experimental conditions. The high performance of DSSCs based on dye 6 among the six dyes explored is attributed to the combined effects of high dye loading on a TiO_2 surface, rapid dye regeneration, and effective retardation of charge recombination.

- One-Step Orthogonal-Bonding Approach to the Self-Assembly of Neutral Rhenium-Based Metallacycles: Synthesis, Structures, Photophysics, and Sensing Applications
  Thanasekaran, P.; Lee, C.-C.; Lu, K.-L. *Acc. Chem. Res.* **2012**, *45*, 1403-1418.
  Abstract:

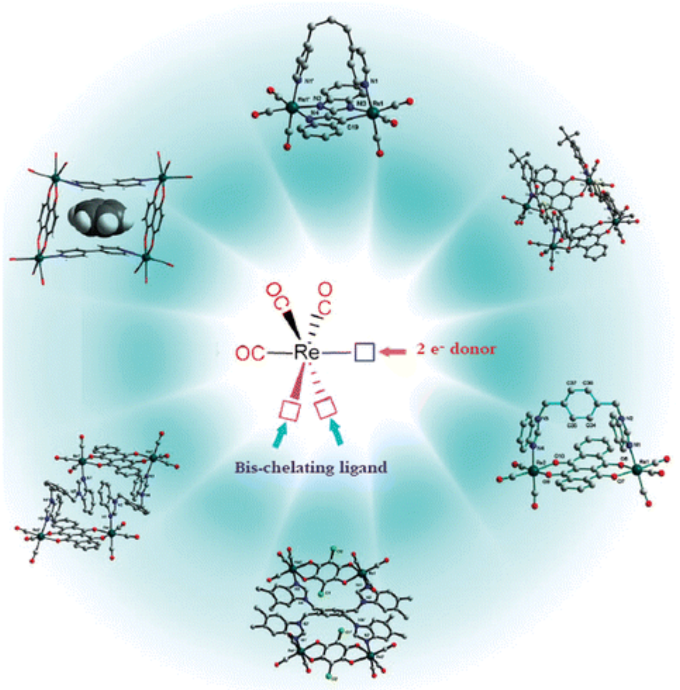

Self-assembled metallacycles offer structural diversity and interesting properties based on their unique frameworks and host–guest chemistry. As a result, the design and synthesis of these materials has attracted significant research interest. This Account describes our comprehensive investigations of an effective orthogonal-bonding approach for the self-assembly of neutral Re-based metallacycles. We discuss the various types of assemblies that can be created based on the nuclearity of the luminophore, including bimetallic materials, rectangles, cages, and calixarenes. This approach permits the preparation of a rectangular molecule, rather than two molecular squares, in excellent yields. We extended this strategy to the high yield synthesis of a series of Re-based metallacycles with different shapes. With the rich spectroscopic and luminescence properties, Re(I) metallacycles provide an excellent platform for studies of host–guest interactions. When possible, we also present potential applications of the luminescent Re-based metallosupramolecular assemblies.

- DNA Block Copolymers: Functional Materials for Nanoscience and Biomedicine
  Schnitzler, T.; Herrmann, A. *Acc. Chem. Res.* **2012**, *45*, 1419-1430.
  Abstract:

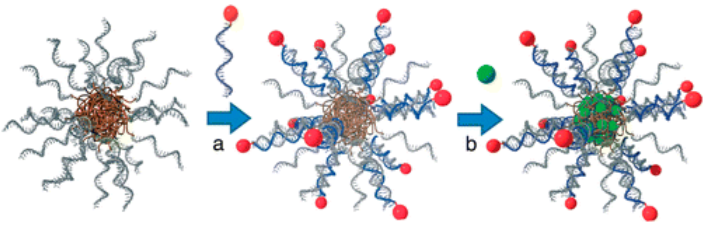

Block copolymers consist exclusively of organic polymers, but researchers are increasingly interested in materials that combine synthetic materials and biomacromolecules. Although many researchers have explored the combination of proteins with organic polymers, far fewer investigations have explored nucleic acid/polymer hybrids, known as DNA block copolymers (DBCs). DNA as a polymer block provides several advantages over other biopolymers. The availability of automated synthesis offers DNA segments with nucleotide precision, which facilitates the fabrication of hybrid materials with monodisperse biopolymer blocks. The directed functionalization of modified single-stranded DNA by Watson–Crick base-pairing is another key feature of DNA block copolymers. Furthermore, the appropriate selection of DNA sequence and organic polymer gives control over the material properties and their self-assembly into supramolecular structures. The introduction of a hydrophobic polymer into DBCs in aqueous solution leads to amphiphilic micellar structures with a hydrophobic polymer core and a DNA corona.

In this Account, we discuss selected examples of recent developments in the synthesis, structure manipulation and applications of DBCs. We present achievements in synthesis of DBCs and their amplification based on molecular biology techniques. We also focus on concepts involving supramolecular assemblies and the change of morphological properties by mild stimuli. Finally, we discuss future applications of DBCs. DBC micelles have served as drug-delivery vehicles, as scaffolds for chemical reactions, and as templates for the self-assembly of virus capsids. In nanoelectronics, DNA polymer hybrids can facilitate size selection and directed deposition of single-walled carbon nanotubes in field effect transistor (FET) devices.

- Characterizing the Photoinduced Switching Process of a Nitrospiropyran Self-Assembled Monolayer Using In Situ Sum Frequency Generation Spectroscopy
  Darwish, T. A.; Tong, Y.; James, M.; Hanley, T. L.; Peng, Q.; Ye, S. *Langmuir* **2012**, *28*, 13852-13860.
  Abstract:

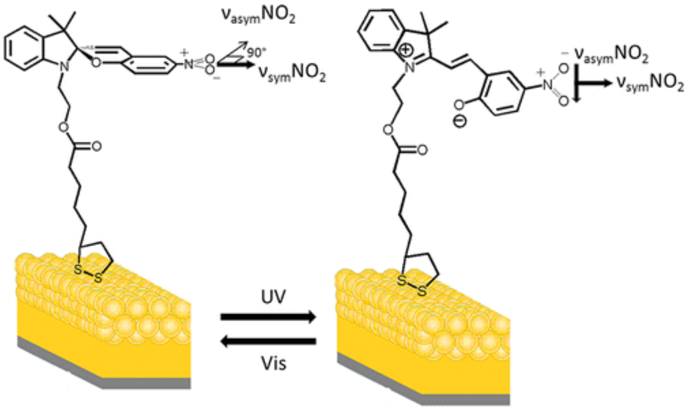

Sum frequency generation (SFG) vibrational spectroscopy is employed to investigate the reversible, photoinduced spiro→merocyanine isomerization of a self-assembled monolayer, the result of attachment of nitrospiropyran to a gold surface using a dithiolane anchoring group. The attachment of these molecular "alligator clips" to spiropyran molecules provide an easily accessible method to self-assemble a robust monolayer of spiropyran on a gold surface, which allows photoswitching of the spiropyran units. Probing the symmetric and antisymmetric stretching modes of the nitro group allows the determination of the structural orientation of the charged moiety with respect to the surface normal as well as the isomerization rates under photoinduced switching conditions. The photoisomerization of the spiropyran SAM on the gold surface is much faster than the rates of switching spiropyrans in a solid crystalline form, and the rate of thermal relaxation of the opened to closed form in this study is found to be on the same time scale as the relaxation of spiropyran when present in solutions with polar solvents.

- Self-Assembled Monolayer Exchange Reactions as a Tool for Channel Interface Engineering in Low-Voltage Organic Thin-Film Transistors
  Lenz, T.; Schmaltz, T.; Novak, M.; Halik, M. *Langmuir* **2012**, *28*, 13900-13904.
  Abstract:

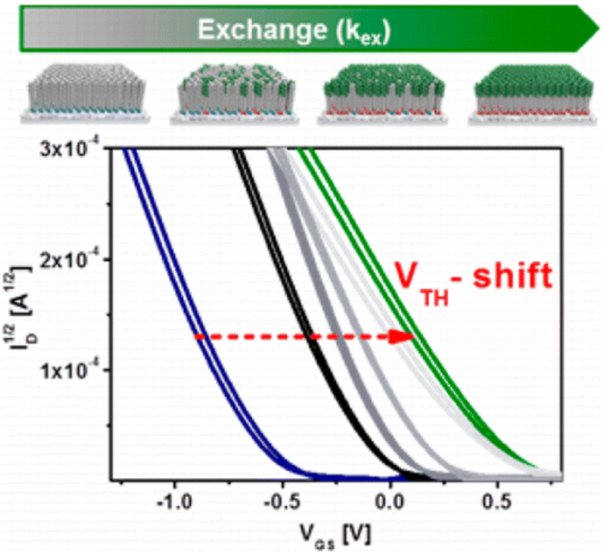

In this work, we compared the kinetics of monolayer self-assembly long-chained carboxylic acids and phosphonic acids on thin aluminum oxide surfaces and investigated their dielectric properties in capacitors and low-voltage organic thin-film transistors. Phosphonic acid anchor groups tend to substitute carboxylic acid molecules on aluminum oxide surfaces and thus allow the formation of mixed or fully exchanged monolayers. With different alkyl chain substituents (*n*-alkyl or fluorinated alkyl chains), the exchange reaction can be monitored as a function of time by static contact angle measurements. The threshold voltage in α,α′-dihexyl-sexithiophene thin-film transistors composed of such mixed layer dielectrics correlates with the exchange progress and can be tuned from negative to positive values or vice versa depending on the dipole moment of the alkyl chain substituents. The change in the dipole moment with increasing exchange time also shifts the capacitance of these devices. The rate constants for exchange reactions determined by the time-dependent shift of static contact angle, threshold voltage, and capacitance exhibit virtually the same value thus proving the exchange kinetics to be highly controllable. In general, the exchange approach is a powerful tool in interface engineering, displaying a great potential for tailoring of device characteristics.

- Generation of 2D organic microsheets from protonated melamine derivatives: suppression of the self assembly of a particular dimension by introduction of alkyl chains
  Xu, J.; Wu, G.; Wang, Z.; Zhang, X. *Chem. Sci.* **2012**, *3*, 3227-3230.
  Abstract:

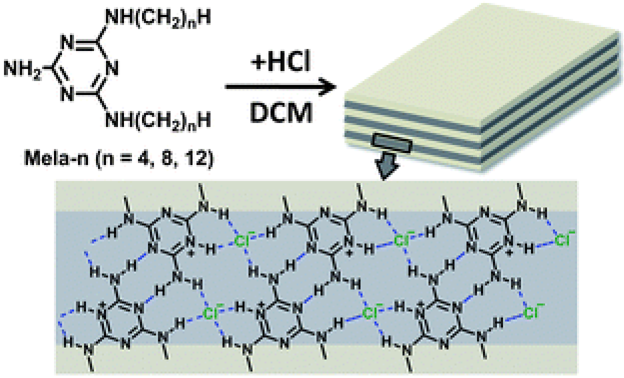

2D organic microsheets are generated from protonated melamine derivatives by suppression of the self assembly of a particular dimension.

- Artificial light-harvesting antenna systems grafted on a carbohydrate platform
  Bonaccorsi, P.; Aversa, M. C.; Barattucci, A.; Papalia, T.; Puntoriero, F.; Campagna, S. *Chem. Commun.* **2012**, *48*, 10550-10552.
  Abstract:

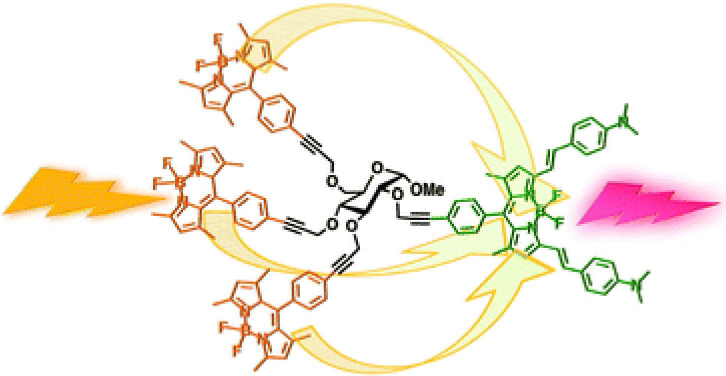

An enantiopure α-D-glucopyranoside derivative has been used as a platform to prepare artificial antenna systems based on bodipy subunits. Efficient and ultrafast energy transfer takes place in the multibodipy systems.

- Dual-mode fluorescence switching induced by self-assembly of well-defined poly(arylene ether sulfone)s containing pyrene and amide moieties
  Park, J.; Kim, J.; Seo, M.; Lee, J.; Kim, S. Y. *Chem. Commun.* **2012,** *48,* 10556–10558.
  Abstract:

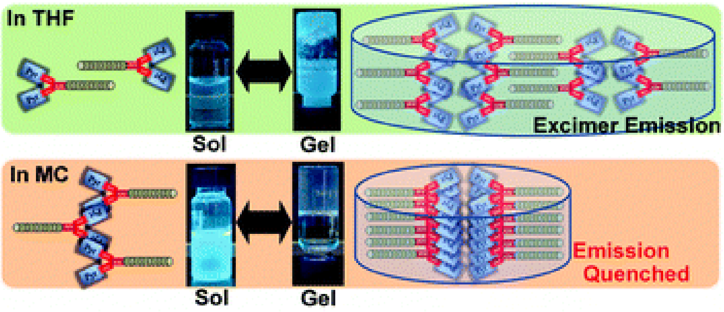

A new class of fluorescent organogelators, pyrene-containing poly(arylene ether sulfone)s, showed two fluorescence switching modes in different gelation solvents. The THF gel exhibited excimer emission due to dimerization of the pyrene groups. In contrast, excimer emission was quenched after gelation in MC because of stacking among the pyrene groups.

- Quencher-free linear probe with multiple fluorophores on an acyclic scaffold
  Asanuma, H.; Akahane, M.; Kondo, N.; Osawa, T.; Kato, T.; Kashida, H. *Chem. Sci.*, **2012,** *3,* 3165–3169.
  Abstract:

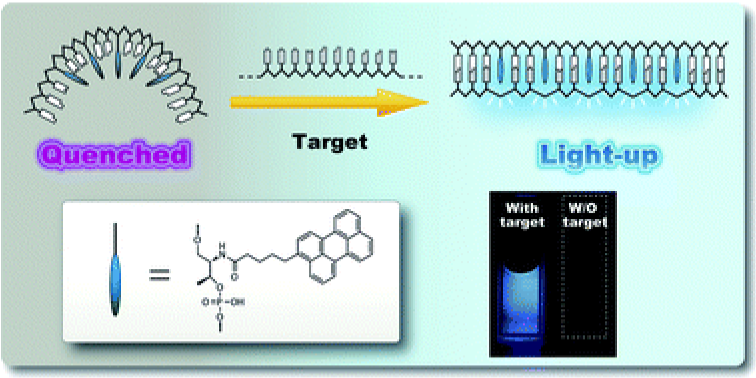

We have developed a new quencher-free stemless linear probe involving multiple perylenes incorporated through D-threoninol; each perylene is separated by intervening natural nucleotides. Without a substrate, the flexible linear probe does not emit fluorescence due to the self-quenching of the weakly interacting fluorophores. Upon hybridization with the target, intercalation of each dye between the base pairs results in emission of strong fluorescence. The maximum signal–background ratio attained was 180, and the response rate was significantly faster than that of a classic hairpin-forming molecular beacon.

- Arrays of giant octagonal and square cylinders by liquid crystalline self-assembly of X-shaped polyphilic molecules
  Liu, F.; Kieffer, R.; Zeng, X.; Pelz, K.; Prehm, M.; Ungar, G.; Tschierske, C. *Nature Communications* **2012**, *3*, 1104.
  Abstract:

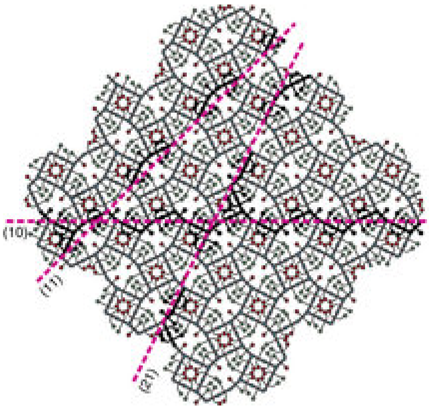

Nanopatterning by molecular self-assembly has been a topic of intense research in pursuit of 'bottom-up' methods of generating structures for use in nanotechnology. The systems most widely studied have been two- and three-dimensional morphologies of block copolymers. However, T- and X-shaped polyphilic liquid crystals have recently been shown to have great potential for generating soft honeycomb-like structures, surpassing those of polymers in both complexity and degree of order. The cell cross-section of the liquid crystals honeycombs has so far been limited by small molecular size. Here we overcome this limitation by exploiting the inability of the polyphiles to simultaneously achieve optimal packing and complete nanophase separation. This frustration results in a two-dimensional periodic honeycomb consisting of giant octagonal and square cylinders with circumferences of 12 and 8 molecules, respectively. In addition to forming large cells, the two-molecule-long bendy walls give this structure extra versatility and stability.

- Protein encapsulation within synthetic molecular hosts
  Fujita, D.; Suzuki, K.; Sato, S.; Yagi-Utsumi, M.; Yamaguchi, Y.; Mizuno, N.; Kumasaka, T.; Takata, M.; Noda, M.; Uchiyama, S.; Kato, K.; Fujita, F. *Nature Communications* **2012**, *3*, 1093.
  Abstract:

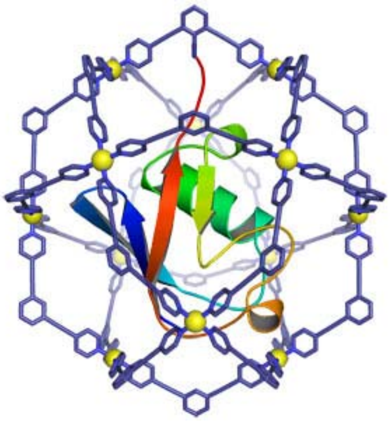

Protein encapsulation has long attracted many chemists and biologists because of its potential to control the structure and functions of proteins, but has been a daunting challenge because of their incommensurably larger size compared with common synthetic hosts. Here we report the encapsulation of a small protein, ubiquitin, within giant coordination cages. The protein was attached to one bidentate ligand and, upon addition of Pd(II) ions (M) and additional ligands (L), $M_{12}L_{24}$ coordination nanocages self-assembled around the protein. Because of the well-defined host framework, the protein-encapsulated structure could be analysed by NMR spectroscopy, ultracentrifugation and X-ray crystallography.

- Kinetically Controlled Nanostructure Formation in Self-Assembled Globular Protein–Polymer Diblock Copolymers
  Thomas, C. S.; Xu, L.; Olsen, B. D. *Biomacromolecules* **2012**, *13*, 2781–2792.
  Abstract:

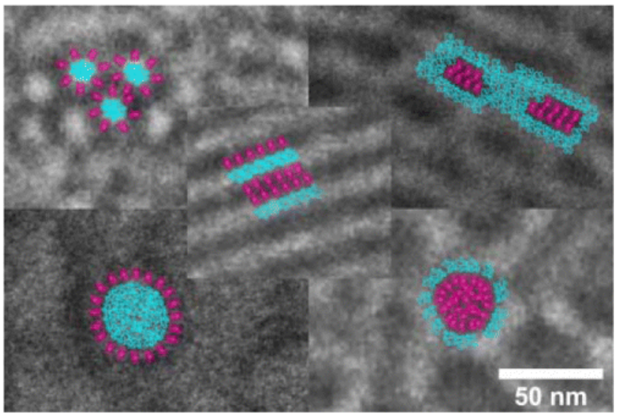

Aqueous processing of globular protein–polymer diblock copolymers into solid-state materials and subsequent solvent annealing enables kinetic and thermodynamic control of nanostructure formation to produce block copolymer morphologies that maintain a high degree of protein fold and function. When model diblock copolymers composed of mCherry-b-poly(N-isopropylacrylamide) are used, orthogonal control over solubility of the protein block through changes in pH and the polymer block through changes in temperature is demonstrated during casting and solvent annealing. Hexagonal cylinders, perforated lamellae, lamellae, or hexagonal and disordered micellar phases are observed, depending on the coil fraction of the block copolymer and the kinetic pathway used for self-assembly. Good solvents for the polymer block produce ordered structures reminiscent of coil–coil diblock copolymers, while an unfavorable solvent results in kinetically trapped micellar structures. Decreasing solvent quality for the protein improves long-range ordering, suggesting that the strength of protein interactions influences nanostructure formation. Subsequent solvent annealing results in evolution of the nanostructures, with the best ordering and the highest protein function observed when annealing in a good solvent for both blocks. While protein secondary structure was found to be almost entirely preserved for all processing pathways, UV–vis spectroscopy of solid-state films indicates that using a good solvent for the protein block enables up to 70% of the protein to be retained in its functional form.

- Structure–Property Evaluation of Thermally and Chemically Gelling Injectable Hydrogels for Tissue Engineering
  Ekenseair, A. K.; Boere, K. W. M.; Tzouanas, S. N.; Vo, T. N.; Kasper, F. K.; Mikos, A. G. *Biomacromolecules* **2012**, *13*, 2821–2830.
  Abstract:

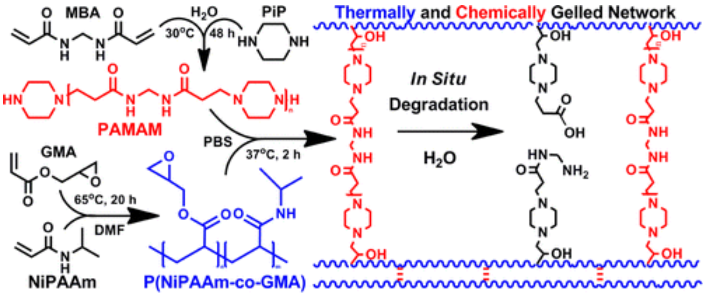

The impact of synthesis and solution formulation parameters on the swelling and mechanical properties of a novel class of thermally and chemically gelling hydrogels combining poly(N-isopropylacrylamide)-based thermogelling macromers containing pendant epoxy rings with polyamidoamine-based hydrophilic and degradable diamine cross-linking macromers was evaluated. Through variation of network hydrophilicity and capacity for chain rearrangement, the often problematic tendency of thermogelling hydrogels to undergo significant syneresis was addressed. The demonstrated ability to tune postformation dimensional stability easily at both the synthesis and formulation stages represents a significant novel contribution toward efforts to utilize poly(N-isopropylacrylamide)-based polymers as injectable biomaterials. Furthermore, the cytocompatibility of the hydrogel system under relevant conditions was established while demonstrating time- and dose-dependent cytotoxicity at high solution osmolality. Such injectable in situ forming degradable hydrogels with tunable water content are promising candidates for many tissue-engineering applications, particularly for cell delivery to promote rapid tissue regeneration in non-load-bearing defects.

- Charge Injection and Transport in Metal-Containing Conducting Polymers: Spectroelectrochemical Mapping of Redox Activities
  Liu, W.; Huang, W.; Chen, C.-H.; Pink, M.; Lee, D. *Chem. Mater.* **2012**, *24*, 3650–3658.
  Abstract:

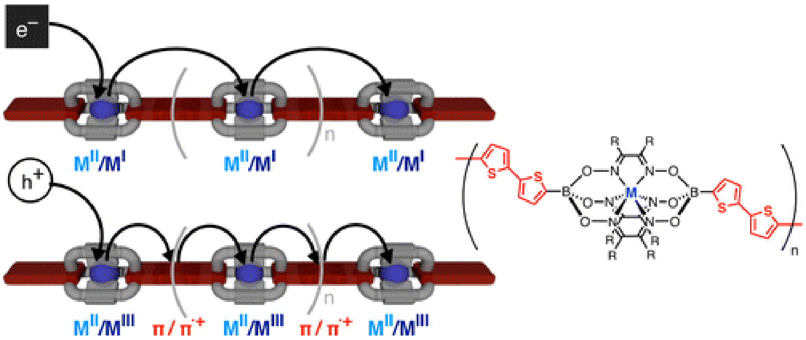

Electropolymerization of tris(dioximate) cage complexes furnished metal-containing conducting polymers (MCPs) that deposit directly onto the electrode surface as uniform films. The injection of electrons into, or removal of electrons from, these electroactive materials proceeds via different pathways with different rates, the underlying molecular mechanisms of which were investigated by a combination of electrochemical, spectroscopic, and focused-ion-beam–scanning electron microscopy (FIB-SEM) cross-section analysis studies. For cobalt-containing polymers, both the metal centers and π-conjugated organic backbone work cooperatively as hopping stations for migrating holes, whereas the reduced polymer utilizes less-efficient self-exchange between cobalt(II) and cobalt(I) centers for electron transport. A small molecule model of such reductively doped polymer was prepared independently, which provided compelling electrochemical and spectroelectrochemical evidence to support the structural integrity of the metal centers upon redox switching. A well-defined metal-to-ligand charge transfer (MLCT) band of the *n*-doped polymer was exploited further as a straightforward spectroscopic tool to quantify the number of redox-active metal centers directly and to estimate the lower distance limit of diffusional charge transport across the bulk material.

- One-Step, Surfactant-Free Hydrothermal Method for Syntheses of Mesoporous TiO2 Nanoparticle Aggregates and Their Applications in High Efficiency Dye-Sensitized Solar Cells
  Cheng, W.-Y.; Deka, J. R.; Chiang, Y.-C.; Rogeau, A.; Lu, S.-Y. *Chem. Mater.* **2012**, *24*, 3255–3262.
  Abstract:

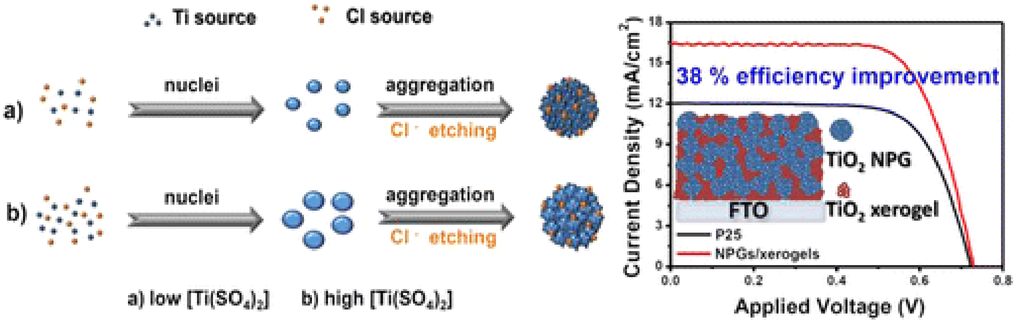

A facile, one-step, template-less, surfactant-free hydrothermal process, using a metal salt as the precursor, is developed to prepare submicrometer sized mesoporous TiO_2 nanoparticle aggregates (NPGs). The as-prepared TiO_2 NPGs are crystalline of the anatase phase, with a high specific surface area of 166 m^2/g, an average pore size of 8.9 nm, and an average NPG size of 840 nm. With these NPGs, a new form of composite photoanode, consisting of the mesoporous TiO_2 NPGs and xerogels, is proposed for high efficiency dye-sensitized solar cells (DSSCs). TiO_2 xerogels are incorporated into the TiO_2 NPGs layer with an impregnation process to form the TiO_2 NPGs/xerogels composite. A high power conversion efficiency of 8.41% is achieved for DSSCs based on the TiO_2 NPGs/xerogels composite photoanode, representing a 38% efficiency boost over the efficiency of 6.11% achieved with a P25 TiO_2 based cell. The success of the present composite TiO_2 nanostructure can be attributed to the effective utilization of the inter-NPG space with the infiltration of the TiO_2 xerogels, the excellent structural connectivity within and across the NPG and xerogel domains for fast electron transport, the high specific surface areas of both the NPGs and xerogels for providing abundant dye adsorption for generation of photoinduced electrons, the formation of a TiO_2 xerogel blocking layer on top of the photoanode substrate, and the submicrometer size of the NPGs for much improved light harvesting efficiency. This new type of composite photoanode, different from the 0D/1D nanostructure based ones, proves effective by taking structural advantages from both constituent nanostructures, the mesoprous NPGs and xerogels, and opens up a new way of thinking in the structural design of the photoanodes.